

PMSM Identification for Automotive Applications: Cancellation of Position Sensor Errors

Nicolas Henwood^{1,2}, Jérémy Malaizé¹, and Laurent Praly²

¹Control, Signal and System Department, IFP New Energy, FRANCE

²Systems and Control Centre, MINES ParisTech, FRANCE

Abstract—The rotor position plays a significant role in identification of motor parameters in Permanent Magnet Synchronous Machines (PMSMs). This paper presents a new model, taking into account errors in measurement of rotor position, for PMSM. A Least Squares (LS) algorithm, based on this new model, is also presented. The proposed algorithm relies on currents, voltages and speed measurements, and identifies both motor parameters and the value of the position error. The method is experimentally implemented and the results demonstrate that the new proposed model and LS algorithm improve the identified resistance and dq-axis inductances, while the rotor flux is hardly affected by the position error. Moreover, a study of measurement uncertainties is conducted to establish confidence intervals on the identified parameters.

I. INTRODUCTION

The emergence of more electric cars is dictated by a growing demand for fuel-efficiency and lower pollutant emissions. The complexity of these green powertrains is accompanied by a significant increase in their cost. To compensate for this side effect, the electric components are expected to operate as close as possible to their optimal performances. Regarding electric machines, this comes down to designing high-level control algorithms to achieve optimal operation. We more specifically believe that three main requirements have to be fulfilled:

- providing the requested torque at any time,
- adjusting the currents within the motor windings to minimize losses,
- ensuring a repeatable response despite the motor heating.

These different objectives may be achieved provided electric machines controllers know of their most significant physical parameters. This paper is more specifically concerned with the identification of Permanent Magnet Synchronous Machines (PMSM), as this technology is widely acknowledged as the best candidate for automotive applications.

The challenge related to the PMSM identification may come from the fact that some parameters undergo changes due to the motor heating. Several solutions may be considered to overcome this issue. The most obvious would consist in putting temperature sensors on the surface of the rotor and in stator windings. However, this expensive solution would not be consistent with mass production. The second way relies on designing a thermal modeling of the motor, based on geometry and physical properties, known heat sources and heat exchanges between the different components. This method allows estimation of the temperature in different parts of the

motor. Many publications on thermal modeling of electric motors can be found in the literature, see [1] for a good review. Nevertheless, using such a model can lead to some issues in the automotive context, where external heat sources may perturb the model.

The last solution consists in directly estimating parameters, namely the winding resistance, the flux due to the magnets and the inductances, to have a precise modeling of PMSM and thus derive high-end control algorithms. Many methods have been proposed to obtain these parameters. For example, [2] designs an observer for magnets flux and [3] determines the winding resistance through current injection. In [4], an online computing method is implemented to identify inductances and resistance while the flux is set to its nominal value. In [5], resistance and inductance are identified through a method based on the Lyapunov stability theorem, while [6] estimates the rotor flux by using a Kalman filter and [7] uses an extended Kalman filter (EKF) to simultaneously identify resistance and flux. See [8] for a good review on parameter estimation of PMSMs.

Our concern is to study the impact of position measurement errors on the identification of PMSM. We shall point out that minor position error may lead to significant deviations of the estimated parameters, which may in turn have some consequences on the performances of the PMSM. This kind of error may appear in several situations, namely when the position sensor is not precise enough, or the position is estimated *via* sensorless schemes or also when slight delays occur within the data acquisition process. This paper presents a new modeling of the PMSM involving this position error. Such a modeling is obtained by applying a rotation to the classical dq-axis frame equations. The available measurements are injected in a least squares (LS) algorithm based on this new modeling. This algorithm is designed to identify the motor parameters whatever the position error value is. The influence of this error on parameter identification can be studied and the actual position error be obtained by minimizing a quadratic index. A testbed allows us to experimentally implement our algorithm and assess its validity. Through these experimentations, we show that motor flux is hardly sensitive to the position error, while the resistance and inductances are highly related to it. Comparisons between identified parameters allowing for position error and not allowing for position error are also made to illustrate the improvements brought by the former. The

dependence of identified parameters on motor speed is also addressed. Moreover, measurement uncertainties are analyzed. For this purpose, measurement noises on current and voltages signals are determined, and their influence on parameter identification is studied to establish confidence intervals on identified parameters.

The structure of this paper is as follows. Section II first presents the classical dq-modeling of the PMSM and the interest in an accurate knowledge of motor parameters for the sake of a high-performance machine control. The new model taking into account the position error is then derived in Section III. In Section IV, we present the LS algorithm used to identify the motor parameters and the position error. Experimental results are finally given in Section V to assess the relevancy of our approach. We then wrap up the paper with some concluding remarks.

II. INFLUENCE OF THE CONTROL ON MOTOR PERFORMANCES

A. PMSM modeling

The classical modeling of salient-pole PMSM in the dq-frame [9] is given by the following set of equations:

$$\begin{aligned} L_d \frac{di_d}{dt} &= -Ri_d + p\omega L_q i_q + v_d \\ L_q \frac{di_q}{dt} &= -Ri_q - p\omega(L_d i_d + \sqrt{\frac{3}{2}}\phi) + v_q \\ \tau &= p\sqrt{\frac{3}{2}}\phi i_q + p(L_d - L_q)i_d i_q \end{aligned} \quad (1)$$

The different parameters appearing in (1) are the stator windings resistance R , the flux due to the rotor magnets ϕ , the inductances (L_d, L_q) modeling saliency and p the number of pole pairs. R and ϕ are temperature dependent parameters, while L_d and L_q are supposed to be constant. (i_d, i_q) and (v_d, v_q) are respectively the currents and input voltages in the dq-axis frame, ω is the rotor shaft's rotation speed and τ the torque provided by the motor. The rotor position ϑ is required to access signals in the dq-axis frame. In the following, we shall assume there is a measurement error ϵ in the position. Let $\hat{i}_d, \hat{i}_q, \hat{v}_d, \hat{v}_q$ be obtained by applying the Park transformation with $\vartheta + \epsilon$. These signals are related through the modeling (4) derived in the following. The remainder of section II is devoted to showing the need for an accurate estimation of the physical parameters in (1) without error in position measurement.

B. Field-Oriented Control of the PMSM

We aim at making the torque τ track a time-varying control demand τ^* . For this purpose, voltages (v_d, v_q) are controlled to make state variables (i_d, i_q) converge to a reference (i_d^*, i_q^*).

For the purposes of control, let us assume we have at our disposal the parameters estimations ($\hat{R}, \hat{\phi}, \hat{L}_d, \hat{L}_q$). These estimations are used to generate the (i_d^*, i_q^*) reference, performed by the following optimization problem [10], which minimizes

copper losses:

$$\begin{aligned} (i_d^*, i_q^*) &= \arg \min_{(i_d, i_q) \in \mathbb{R}^2} (i_d^2 + i_q^2) \\ \text{s.t.:} \quad & \text{(i)} \quad \tau^* = p\sqrt{\frac{3}{2}}\hat{\phi}i_q + p(\hat{L}_d - \hat{L}_q)i_d i_q \\ & \text{(ii)} \quad i_d^2 + i_q^2 \leq i_{\max}^2 \\ & \text{(iii)} \quad v_d^2 + v_q^2 \leq v_{\max}^2 \end{aligned} \quad (2)$$

where (iii) is given by equations (1) in steady state, i_{\max} comes from thermal considerations and v_{\max} from technological constraints (maximum voltage deliverable by the DC bus). Equations in (2) highlight that the optimization solution highly depends on the parameters estimation.

C. Influence of temperature on the control performances

To illustrate the impact of a good knowledge of temperature dependent parameters on motor performances, let us consider the Toyota Prius electric motor, documented in [11]. We assume this motor has been heated to 120°C. Figure 1 then shows the maximum torque and power available according to the motor speed in two cases. In the first one, values of \hat{R} and $\hat{\phi}$ at 20°C are used in the optimization problem (2), whereas in the second one, the actual values at 120°C are used in (2). Figure 1 attests that the knowledge of the temperature updated values of \hat{R} and $\hat{\phi}$ extends the operating range. At low speed, the maximum available torque is indeed increased by 10%, while a rise of 10% is also noticed for maximum available power at high speed. This possible performances improvement motivates the need for an accurate estimation of the two temperature dependent parameters \hat{R} and $\hat{\phi}$, which requires a strong knowledge of the rotor position.

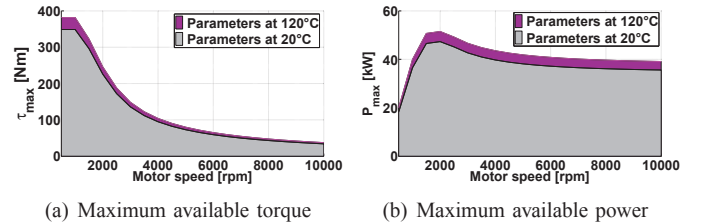


Fig. 1. Influence of control on performances

III. DERIVATION OF THE NEW MODEL

Let us return to the case where $\epsilon \neq 0$. We choose to perform the identification in the rotating frame with bias ϵ . Our goal is to derive a new model linking (\hat{i}_d, \hat{i}_q) to (\hat{v}_d, \hat{v}_q).

To that end, let us apply an inverse rotation of angle ϑ to currents and voltages of the classical dq-model (1) to get the model in the $\alpha\beta$ -axis frame. Then, applying a direct rotation of angle $\vartheta + \epsilon$ to currents and voltages in this $\alpha\beta$ -model leads to the new modeling we are looking for. Considering only the currents case, we eventually come up with:

$$\begin{pmatrix} \hat{i}_d \\ \hat{i}_q \end{pmatrix} = \begin{pmatrix} \cos \epsilon & \sin \epsilon \\ -\sin \epsilon & \cos \epsilon \end{pmatrix} \begin{pmatrix} i_d \\ i_q \end{pmatrix} \quad (3)$$

The same transformation applies to (\hat{v}_d, \hat{v}_q) and (v_d, v_q).

$$\begin{aligned}
L_d L_q \frac{d\hat{i}_d}{dt} &= \hat{v}_d(L_q \cos^2 \epsilon + L_d \sin^2 \epsilon) + \hat{v}_q(L_d - L_q) \frac{\sin 2\epsilon}{2} + \hat{i}_d \left(-R(L_q \cos^2 \epsilon + L_d \sin^2 \epsilon) + p\omega(L_q^2 - L_d^2) \frac{\sin 2\epsilon}{2} \right) \\
&+ \hat{i}_q \left(R(L_q - L_d) \frac{\sin 2\epsilon}{2} + p\omega(L_q^2 \cos^2 \epsilon + L_d^2 \sin^2 \epsilon) \right) - p\omega L_d \sqrt{\frac{3}{2}} \phi \sin \epsilon \\
L_d L_q \frac{d\hat{i}_q}{dt} &= \hat{v}_d(L_d - L_q) \frac{\sin 2\epsilon}{2} + \hat{v}_q(L_q \sin^2 \epsilon + L_d \cos^2 \epsilon) + \hat{i}_d \left(R(L_q - L_d) \frac{\sin 2\epsilon}{2} - p\omega(L_q^2 \sin^2 \epsilon + L_d^2 \cos^2 \epsilon) \right) \\
&+ \hat{i}_q \left(-R(L_q \sin^2 \epsilon + L_d \cos^2 \epsilon) + p\omega(L_d^2 - L_q^2) \frac{\sin 2\epsilon}{2} \right) - p\omega L_d \sqrt{\frac{3}{2}} \phi \cos \epsilon
\end{aligned} \tag{4}$$

Applying the change of coordinates (3) to equations (1) leads to (4). Note that these equations may be found in [12], though not used for the same purposes. For the sake of simplicity, the expression of τ is omitted. In steady-state, equations (4) can also be expressed as follows:

$$\begin{aligned}
\hat{v}_{dq} &= p\omega \sqrt{\frac{3}{2}} \phi \begin{pmatrix} \sin \epsilon \\ \cos \epsilon \end{pmatrix} + \\
&\begin{pmatrix} R + p\omega(L_d - L_q) \frac{\sin 2\epsilon}{2} & -p\omega(L_q \cos^2 \epsilon + L_d \sin^2 \epsilon) \\ p\omega(L_d \cos^2 \epsilon + L_q \sin^2 \epsilon) & R - p\omega(L_d - L_q) \frac{\sin 2\epsilon}{2} \end{pmatrix} \hat{i}_{dq}
\end{aligned} \tag{5}$$

with $\hat{v}_{dq} = (\hat{v}_d \ \hat{v}_q)^T$ and $\hat{i}_{dq} = (\hat{i}_d \ \hat{i}_q)^T$.

If $\epsilon = 0$, it is easy to verify we get equations (1) in steady-state. Therefore, comparisons between results obtained with classical or new modeling are easy to make.

IV. LS ALGORITHM FOR MOTOR PARAMETERS IDENTIFICATION AND POSITION ERROR DETERMINATION

The following procedure, performed offline, is followed to identify the motor parameters and determine the position error when the new modeling exposed in (4) and (5) is used.

Procedure . *Provided ω , \hat{v}_{dq} and \hat{i}_{dq} are known, an estimate of the position measurement error ϵ is given by the following one-dimensional optimization problem:*

$$\hat{\epsilon} = \arg \min_{\epsilon} \left(\min_{\Theta} \|y - \Psi(\epsilon)\Theta\|^2 \right) \tag{6}$$

with y and $\Psi(\epsilon)$ respectively given by (11) and (12). By doing so, estimates of the physical parameters in (1) may be obtained via

$$\hat{\Theta} = (\hat{R}, \hat{\phi}, \hat{L}_d, \hat{L}_q)^T = \Theta^*(\hat{\epsilon}) \tag{7}$$

with the function Θ^* given by:

$$\Theta^*(\epsilon) = \arg \min_{\Theta} \|y - \Psi(\epsilon)\Theta\|^2 = (\Psi^T(\epsilon)\Psi(\epsilon))^{-1} \Psi^T(\epsilon)y \tag{8}$$

Steady-state modeling (5) is used throughout the identification process and these equations are linear in $\Theta = (R, \phi, L_d, L_q)^T$ and nonlinear in ϵ . A LS algorithm is applied to identify Θ for any ϵ in a reasonable range around zero,

assuming the position measurement error is small. Let us rewrite (5):

$$\begin{aligned}
\hat{v}_d &= (\alpha_d(\epsilon) + \beta_d(\epsilon)\hat{i}_d + \gamma_d(\epsilon)\hat{i}_q)\Theta \\
\hat{v}_q &= (\alpha_q(\epsilon) + \beta_q(\epsilon)\hat{i}_d + \gamma_q(\epsilon)\hat{i}_q)\Theta
\end{aligned} \tag{9}$$

with

$$\begin{aligned}
\alpha_d(\epsilon) &= \begin{pmatrix} 0 & p\omega \sqrt{\frac{3}{2}} \sin \epsilon & 0 & 0 \end{pmatrix} \\
\alpha_q(\epsilon) &= \begin{pmatrix} 0 & p\omega \sqrt{\frac{3}{2}} \cos \epsilon & 0 & 0 \end{pmatrix} \\
\beta_d(\epsilon) &= \begin{pmatrix} 1 & 0 & p\omega \frac{\sin 2\epsilon}{2} & -p\omega \frac{\sin 2\epsilon}{2} \end{pmatrix} \\
\gamma_d(\epsilon) &= \begin{pmatrix} 1 & 0 & -p\omega \frac{\sin 2\epsilon}{2} & p\omega \frac{\sin 2\epsilon}{2} \end{pmatrix} \\
\beta_q(\epsilon) &= \begin{pmatrix} 0 & 0 & p\omega \cos^2 \epsilon & p\omega \sin^2 \epsilon \end{pmatrix} \\
\gamma_q(\epsilon) &= - \begin{pmatrix} 0 & 0 & p\omega \sin^2 \epsilon & p\omega \cos^2 \epsilon \end{pmatrix}
\end{aligned} \tag{10}$$

with ω constant during the identification process. In our purely static context, Θ and ϵ can be extracted from a sufficient number of copies of (9) obtained by varying the constant values of $\hat{i}_d, \hat{i}_q, \hat{v}_d$ and \hat{v}_q . This motivates us to control currents to successive constant setpoints. For each of these steps, mean values of currents $\langle \hat{i}_j \rangle^{(i)}$ and voltages $\langle \hat{v}_j \rangle^{(i)}$, $j = d, q$, are computed once in steady-state. Assuming there are N steps of (\hat{i}_d, \hat{i}_q) in input, N copies linking currents, voltages and parameters are made available, leading to $2N$ equations. Let y be the vector of the mean voltages measured on every step:

$$y = \begin{pmatrix} \langle \hat{v}_d \rangle^{(1)} \\ \vdots \\ \langle \hat{v}_d \rangle^{(N)} \\ \langle \hat{v}_q \rangle^{(1)} \\ \vdots \\ \langle \hat{v}_q \rangle^{(N)} \end{pmatrix} \tag{11}$$

and $\Psi(\epsilon)$ be given by:

$$\Psi(\epsilon) = \begin{pmatrix} \alpha_d(\epsilon) + \beta_d(\epsilon) \langle \hat{i}_d \rangle^{(1)} + \gamma_d(\epsilon) \langle \hat{i}_q \rangle^{(1)} \\ \vdots \\ \alpha_d(\epsilon) + \beta_d(\epsilon) \langle \hat{i}_d \rangle^{(N)} + \gamma_d(\epsilon) \langle \hat{i}_q \rangle^{(N)} \\ \alpha_q(\epsilon) + \beta_q(\epsilon) \langle \hat{i}_d \rangle^{(1)} + \gamma_q(\epsilon) \langle \hat{i}_q \rangle^{(1)} \\ \vdots \\ \alpha_q(\epsilon) + \beta_q(\epsilon) \langle \hat{i}_d \rangle^{(N)} + \gamma_q(\epsilon) \langle \hat{i}_q \rangle^{(N)} \end{pmatrix} \quad (12)$$

Then, for all ϵ , the least squares algorithm gives the best parameter vector (8). Position error $\hat{\epsilon}$ is then chosen to be the one minimizing the cost function (6) and identified motor parameters are thus given by (7).

V. RESULTS

A. Experimental setup

The previously described identification method is experimentally validated on a testbed made up of two PMSM, connected through a shaft. This setup is illustrated in figure 2. These two drives have respective rated power of 1.7kW and 2.2kW, and similar rated speed of 6000rpm. The former is intended to deliver a desired torque, while the latter is intended to control the rotation speed of the shaft. Table I presents the values of the first motor parameters, which will be used as benchmarks in this section. Inductances values are those given by the technical datasheet, which does not distinguish between the direct and quadrature inductance. The value of the resistance is obtained by applying a constant voltage to the windings, with a locked rotor, and monitoring the resulting current. Finally, back-emf measurements under zero current enable us to find the value of the flux. All of these parameter values are the reference values that our identified parameters will be compared to, though some *a priori* doubts may be expressed about the reference values of the inductances.



Fig. 2. Experimental setup

TABLE I
ELECTRIC MOTOR PARAMETERS

p	R (20°C)	ϕ (20°C)	L_d	L_q
3	0.2525 Ω	0.0728 Wb	0.77 mH	0.77 mH

B. Parameters identification

The experimental results of parameters identification at 1000 rpm are given in figure 3. On each curve, results with classical ($\epsilon = 0$, triangle) and new ($\epsilon = \hat{\epsilon}$, circle) modeling are compared. Figure 3(a) presents the cost function to be minimized to find the optimal position error $\hat{\epsilon}$, given by (6). We clearly see that taking account of the position error makes

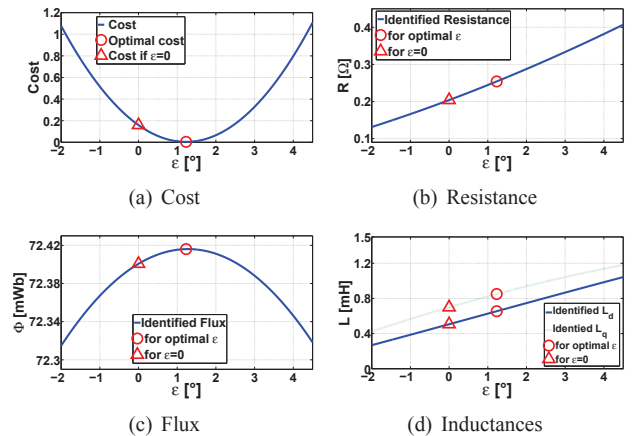


Fig. 3. Cost and identified parameters according to position error (1000 rpm)

it possible to greatly reduce the cost and so, to improve parameter identification. In this particular case, cost is indeed divided by almost 40. Figures 3(b) to 3(d) show the values of identified motor parameters according to position error. The function Θ^* is actually evaluated for any ϵ within the chosen range on these figures. We notice that an error of a few degrees in position leads to significant identification errors, in particular for resistance and inductances identification. In the presented case for instance, the new modeling leads to improvements of 24%, 29% and 21% on resistance, direct and quadrature inductances identification respectively. Concerning the flux identification, the dependence on position error is less marked, but still exists.

Figure 4 presents identified parameters dependence on motor speed. We first notice a decreasing trend in the position error according to the speed in figure 4(a). Figures 4(b) to 4(e) show a comparison of the identified parameters as a function of the speed, whether the position error is taken into account or not. The classical modeling results are represented by triangles and new modeling ones by circles. There is no significant improvement in the identification of the flux. On the contrary, differences are far more important for the other parameters. With the classical modeling, identified resistance and inductances vary greatly with speed, which is not consistent with physical properties of materials. With the new modeling, there still exists a small dependence on speed, especially concerning resistance, but it is much less pronounced.

C. Measurement uncertainties

The results presented in the previous part were obtained by applying the LS algorithm to mean values of currents and voltages. In fact, (13) and (14) show the dependence of y (11)

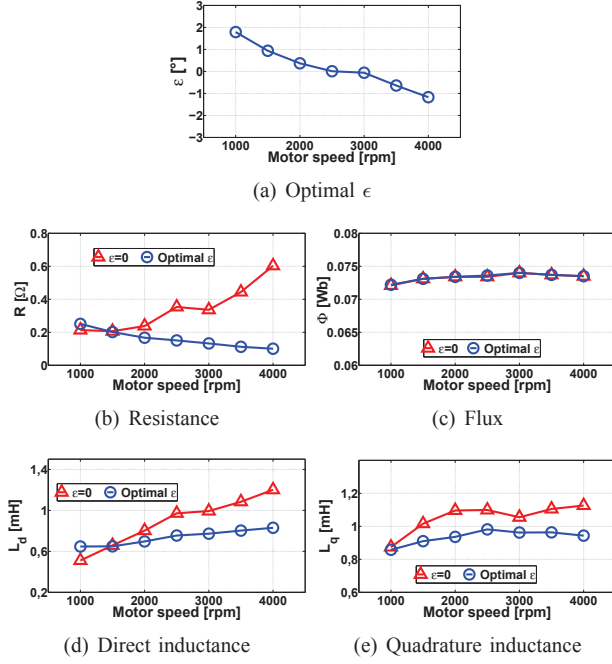


Fig. 4. Identified parameters according to motor speed

and $\Psi(\epsilon)$ (12) on these mean values:

$$y \left(\left\{ \langle \hat{v}_d \rangle^{(i)}, \langle \hat{v}_q \rangle^{(i)} \right\}_{1 \leq i \leq N} \right) \quad (13)$$

$$\Psi \left(\epsilon, \left\{ \langle \hat{i}_d \rangle^{(i)}, \langle \hat{i}_q \rangle^{(i)} \right\}_{1 \leq i \leq N} \right) \quad (14)$$

However, since we are dealing with experimental data, the mean values are subject to measurement uncertainties and thus the identified parameters are subject to estimation errors.

In this part, the influence of a wrong knowledge of currents and voltages mean values on identified parameters is studied through a Monte Carlo statistical analysis. To that end, the LS algorithm will be applied to noisy mean values. For the sake of simplicity, let us consider the case of the signal \hat{i}_q , the same notations and approach being applicable to \hat{i}_d , \hat{v}_d and \hat{v}_q . Let r_{iq} be the measurement noise on the instantaneous signal \hat{i}_q and $\delta_{iq}^{(i)}$ the noise on the mean value $\langle \hat{i}_q \rangle^{(i)}$ of the signal \hat{i}_q on the i -th step.

Our Monte Carlo statistical analysis requires the knowledge of the characteristics of the stochastic process generating the measurement noise. Since we only have a record of this noise, we rely on ergodicity to approximate these characteristics. This leads us to assume that each measurement noise is generated by independent and identically distributed random variables. In this case, it follows from [13, Theorem 36.4] for instance that the statistical properties of each noise can be approximated by its time statistics, provided the time window for doing this estimation is long enough.

We first determine the temporal distribution, presented in figure 5, of the noise r_{iq} , which can thus be considered as its statistic distribution. To obtain this distribution, the noise on each abc-current, is determined by eliminating from the time signal its mean value and all of its frequency components

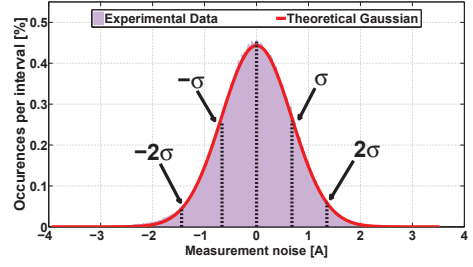


Fig. 5. Temporal distribution of noise r_{iq}

which are not related to the noise. These components, determined by an FFT, mostly include fundamental and some harmonics frequencies induced by the back-emf and the inverter switches. Furthermore, the noises on currents (and voltages) in the abc-axis frame are independent. r_{iq} is then obtained through the Park transformation.

Assuming this distribution is normal, we determine its standard deviation (SD) σ . Vertical lines indicate positions of -2σ , $-\sigma$, mean value (i.e. zero), σ and 2σ . Moreover, the Gaussian curve with variance σ^2 and zero mean is plotted to make sure it fits with the distribution.

Now looking for the statistical distribution of the noise $\delta_{iq}^{(i)}$ on the mean value $\langle \hat{i}_q \rangle^{(i)}$, let L be the length of the i -th step. Then, under the previously made assumptions, $\delta_{iq}^{(i)}$ follows a normal distribution with zero mean and variance σ^2/L [14, Theorem 3.2.4]. Table II summarizes SDs of noises on mean values on any step i for each current and voltage, at 1000 rpm.

TABLE II
STANDARD DEVIATIONS OF NOISES ON MEAN VALUES

Signal	$\delta_{id}^{(i)}$	$\delta_{iq}^{(i)}$	$\delta_{vd}^{(i)}$	$\delta_{vq}^{(i)}$
SD : σ/\sqrt{L}	1.5 mA	1.0 mA	17 mV	28 mV

Knowing these statistical properties, the Monte Carlo analysis can now be performed: let us apply several times the LS algorithm described in section IV, with (15) and (16) replacing (11) and (12):

$$y \left(\left\{ \langle \hat{v}_d \rangle^{(i)} + \delta_{vd}^{(i)}, \langle \hat{v}_q \rangle^{(i)} + \delta_{vq}^{(i)} \right\}_{1 \leq i \leq N} \right) \quad (15)$$

$$\Psi \left(\epsilon, \left\{ \langle \hat{i}_d \rangle^{(i)} + \delta_{id}^{(i)}, \langle \hat{i}_q \rangle^{(i)} + \delta_{iq}^{(i)} \right\}_{1 \leq i \leq N} \right) \quad (16)$$

where $(\delta_{id}^{(i)}, \delta_{iq}^{(i)}, \delta_{vd}^{(i)}, \delta_{vq}^{(i)}, i = 1 \dots N)$ are randomly generated according to normal distributions with zero mean and SD given in table II. Figure 6 presents the resulting identified parameters distributions, obtained via 35000 independent trial runs. Let us assume these distributions are also Gaussian. Table III presents, for each parameter distribution, its mean value, SD and 95% confidence interval (CI). We are also interested in determining the identification algorithm accuracy, depending on the identification bias and the measurement uncertainties. We introduce a normalized mean error (NME) computed as follows for R . The same approach holds for other parameters. With R the reference value of the resistance (cf. table I) and

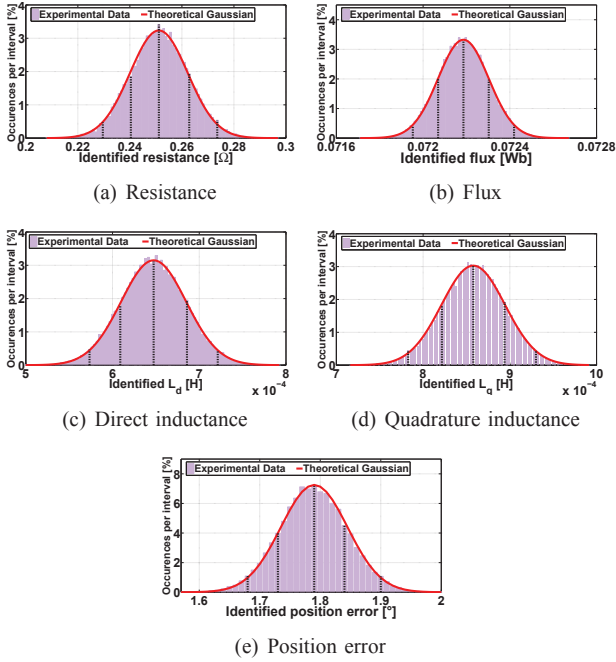


Fig. 6. Identified parameters distributions at 1000 rpm

\hat{R} the identified mean value:

$$NME = \frac{\sqrt{MSE}}{R} \quad (17)$$

where MSE stands for the mean square error:

$$MSE(\hat{R}) = E((\hat{R} - R)^2) = Var(\hat{R}) + (Bias(\hat{R}, R))^2 \quad (18)$$

The results are presented for both the classical modeling (white background) and the new modeling (grey background). We notice that the uncertainties due to noise are quite similar

TABLE III
IDENTIFIED PARAMETERS CHARACTERISTICS

Parameter	ϵ	Mean	SD	95% CI	NME
$R[\Omega]$	$\epsilon = \hat{\epsilon}$	0.2511	0.0111	0.2294 - 0.2728	4.4%
	$\epsilon = 0$	0.1774	0.0108	0.1562 - 0.1987	30.0%
$\phi[mWb]$	$\epsilon = \hat{\epsilon}$	72.19	0.117	71.96 - 72.41	0.86%
	$\epsilon = 0$	72.15	0.116	71.92 - 72.38	0.91%
$L_d[mH]$	$\epsilon = \hat{\epsilon}$	0.6474	0.0375	0.5740 - 0.7208	16.6%
	$\epsilon = 0$	0.4293	0.0385	0.3538 - 0.5047	44.5%
$L_q[mH]$	$\epsilon = \hat{\epsilon}$	0.8578	0.0366	0.7861 - 0.9296	12.4%
	$\epsilon = 0$	0.6424	0.0357	0.5724 - 0.7124	17.2%
$\epsilon[^\circ]$	$\epsilon = \hat{\epsilon}$	1.79	0.055	1.682 - 1.898	

with both models, standard deviations and thus the width of confidence intervals being very close. Furthermore, if noise has a non-negligible impact on resistance and inductances identification, the flux identification is hardly affected by it. Finally, focusing on the normalized mean errors shows us that the new modeling brings a very significant improvement on resistance identification. An important improvement can also be noticed on inductances identification, even if error rates remain high because of the obvious distinction between L_d and L_q , which is not taken into account in the technical datasheet of the motor. Thus, NME of inductances may be smaller.

VI. CONCLUSION

The new modeling, combined with its dedicated LS algorithm, enables great improvements in resistance and inductances identification, whatever the speed is, and to determine the position error. With flux being less sensitive to a position error than the three other parameters, flux identification results are quite similar with classical and new modelings. The parameters uncertainties study shows that, despite measurement noise, we can be very confident in the flux identification. Concerning resistance and inductances identification, we must be more careful, since slight errors remain after the identification process. We also notice that resistance identification, and to a lesser extent inductances identification, still depends a little on speed. Future work will consist in trying to further improve the modeling to get rid of this speed dependency, and to build an observer based on this new modeling to get an accurate online estimation of temperature dependent parameters and as a result, be able to reach the three main objectives we mentioned in the introduction.

REFERENCES

- [1] G. Demetriades, H. de la Parra, E. Andersson, and H. Olsson, "A real-time thermal model of a permanent-magnet synchronous motor," *Power Electronics, IEEE Transactions on*, vol. 25, no. 2, pp. 463–474, 2010.
- [2] A. Specht and J. Böcker, "Observer for the rotor temperature of IPMSM," in *Power Electronics and Motion Control Conference (EPE/PEMC), 2010 14th International*. IEEE, pp. T4–12.
- [3] S. Wilson, P. Stewart, and B. Taylor, "Methods of resistance estimation in permanent magnet synchronous motors for real-time thermal management," *Energy Conversion, IEEE Transactions on*, vol. 25, no. 3, pp. 698–707, 2010.
- [4] S. Moreau, R. Kahoul, and J. Louis, "Parameters estimation of permanent magnet synchronous machine without adding extra-signal as input excitation," in *Industrial Electronics, 2004 IEEE International Symposium on*, vol. 1. IEEE, 2004, pp. 371–376.
- [5] L. Liu and D. Cartes, "Synchronisation based adaptive parameter identification for permanent magnet synchronous motors," *Control Theory & Applications, IET*, vol. 1, no. 4, pp. 1015–1022, 2007.
- [6] X. Xiao, C. Chen, and M. Zhang, "Dynamic Permanent Magnet Flux Estimation of Permanent Magnet Synchronous Machines," *Applied Superconductivity, IEEE Transactions on*, vol. 20, no. 3, pp. 1085–1088, 2010.
- [7] Z. Zhu, X. Zhu, P. Sun, and D. Howe, "Estimation of winding resistance and PM flux-linkage in brushless AC machines by reduced-order extended Kalman Filter," in *Networking, Sensing and Control, 2007 IEEE International Conference on*. IEEE, pp. 740–745.
- [8] K. Liu, Q. Zhang, J. Chen, Q. Zhu, J. Zhang, and A. Shen, "Online Multi-parameter Estimation of Non-salient Pole PM Synchronous Machines with Temperature Variation Tracking," *Industrial Electronics, IEEE Transactions on*, vol. 58, no. 99, pp. 1776–1788, 2010.
- [9] J. Chiasson, *Modeling and High-Performance Control of Electric Machines*. IEEE Press, 2005.
- [10] J. Malaize, W. Dib, and S. Toru, "Adaptive torque control of permanent magnet synchronous motors in automotive applications," in *Vehicle Power and Propulsion Conference*, Lille, September 2010.
- [11] R. Staunton, C. Ayers, L. Marlino, J. Chiasson, and T. Burress, "Evaluation of 2004 Toyota Prius hybrid electric drive system," *Oak Ridge National Laboratory Technical Report, ORNL/TM-2006/423*, 2006.
- [12] V. Petrovi and A. Stankovic, "Modeling of pm synchronous motors for control and estimation tasks," in *Decision and Control, 2001. Proceedings of the 40th IEEE Conference on*, vol. 3. IEEE, 2001, pp. 2229–2234.
- [13] P. Billingsley, *Probability and measure. Third Edition*. John Wiley & Sons, 1995.
- [14] Y. Linnik, *Méthode des moindres carrés*. Dunod, 1963.